



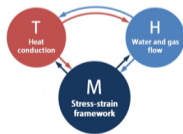
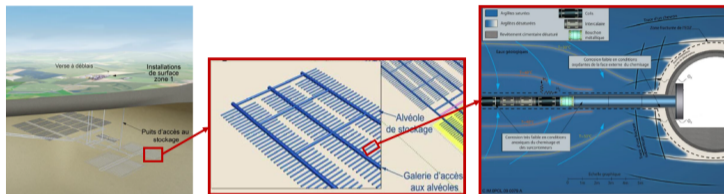
Numerical modeling of cracking with thermo-hydro-mechanical process considering rock heterogeneity

Z. Yu (University of Lille), M. Wang (University of Lille), M.N. Vu (Andra), J.F. Shao* (University of Lille)

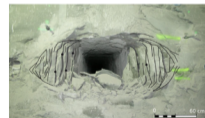
27 May, 2021

Study background

Study supported by ANDRA (French national radioactive waste management agency)



THM coupling behaviors



Damage/cracking behaviors

- Section 1 : A modified phase field method
 - Introduction of phase field method
 - Phase field method based on tensile and shear damage
- Section 2 : THM coupling with phase field method
- Section 3 : Examples of application
 - Thermal extension tests
 - Excavation induced crack zone around GCS gallery
 - Heating induced crack in ALC heating test

Section 1 : A modified phase field method

Introduction of phase field method

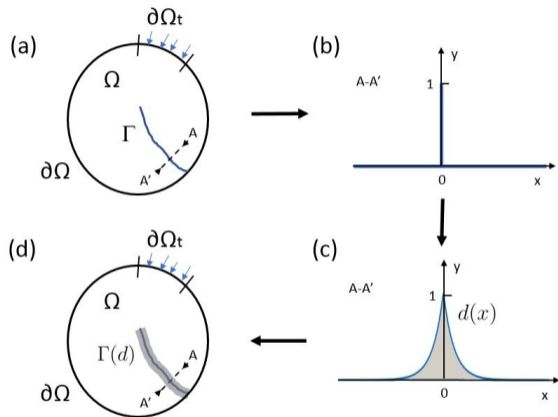


FIGURE – (a) The real sharp crack Γ in the solid Ω ; (b) The real sharp crack in the 1-D coup $A-A'$; (c) The diffused crack by Phase-field in the 1-D coup $A-A'$; (d) The diffused crack with its equivalent surface $\Gamma(d)$.

Diffusive crack function :

$$d(x) = e^{-\frac{|x|}{l_d}} \quad (1)$$

Equivalent crack surface :

$$\Gamma(d) = \int_{-\infty}^{+\infty} \frac{1}{2} \left(\frac{1}{l_d} d^2 + l_d d'^2 \right) dx = \int_{-\infty}^{+\infty} \gamma(d, \nabla d) dx \quad (2)$$

The minimisation of the energy functional :

$$E(u, d) = \int_{\Omega} g(d) \Psi_0(\varepsilon(u)) dV + g_c \int_{\Omega} \gamma(d, \nabla d) dV \quad (3)$$

Section 1 : A modified phase field method

Phase field method based on tensile and shear crack

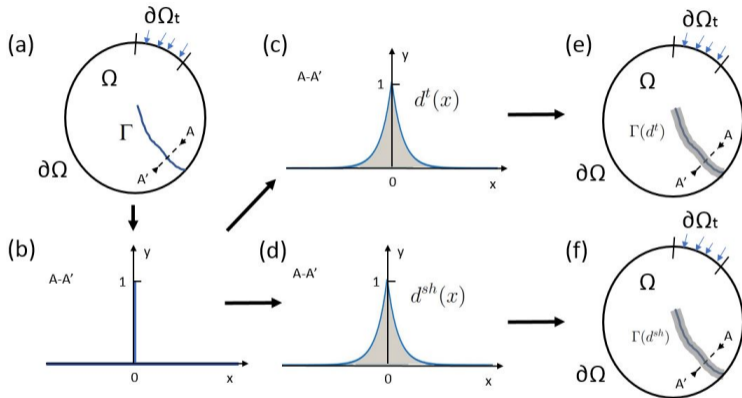


FIGURE – (a) The real sharp crack Γ in the solid Ω ; (b) The real sharp crack in the 1-D coup $A-A'$; (c) and (d) The diffused tensile & shear crack by phase field method in the 1-D coup $A-A'$; (e) and (f) The diffused tensile & shear crack with its equivalent surface $\Gamma(d^t)$ & $\Gamma(d^{sh})$.

Section 1 : A modified phase field method

The new modified phase-field model is defined by two types of damage d^t and d^{sh} . The minimisation of the energy functional is rewritten as :

$$\begin{aligned} E(u, d) = & \underbrace{\int_{\Omega} \Psi(\varepsilon(u), d^t, d^{sh}) dV}_{\text{stored energy}} \\ & + \underbrace{g_c^t \int_{\Omega} \gamma_t(d^t, \nabla d^t) dV}_{\text{tensile fracture energy}} + \underbrace{g_c^{sh} \int_{\Omega} \gamma_{sh}(d^{sh}, \nabla d^{sh}) dV}_{\text{shear fracture energy}} \end{aligned} \quad (4)$$

Following the thermodynamic theory, the damage criterion can be written as :

$$\begin{cases} f^t = -\frac{\partial W}{\partial d^t} = -\frac{\partial \Psi(\varepsilon, d^t, d^s)}{\partial d^t} - g_c^t \left(\frac{d^t}{l_d} - l_d \Delta d^t \right) \leq 0 \\ f^s = -\frac{\partial W}{\partial d^s} = -\frac{\partial \Psi(\varepsilon, d^t, d^s)}{\partial d^s} - g_c^s \left(\frac{d^s}{l_d} - l_d \Delta d^s \right) \leq 0 \end{cases} \quad (5)$$

Section 2 : THM coupling with phase field method

The pore pressure field

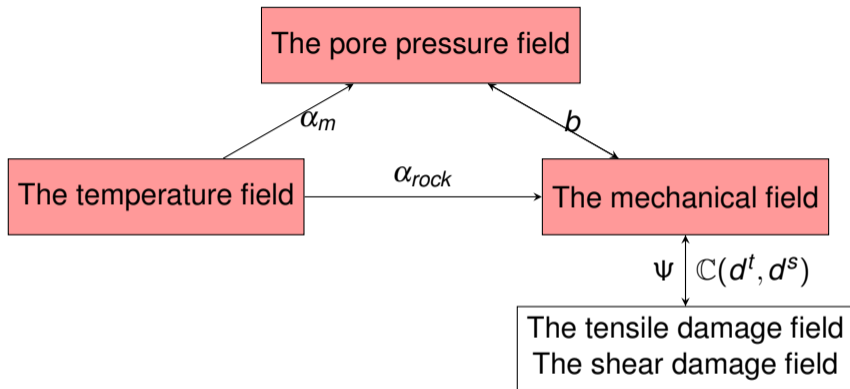
The temperature field

The mechanical field

The tensile damage field
The shear damage field

- The pore pressure field : $[R_h](P) = (f_h)$
- The temperature field : $[R_T](T) = (f_T)$
- The mechanical field : $[R_m](u) = (F_m)$
- The tensile damage field : $[R_{dt}](d^t) = (f_{dt})$
- The shear damage field : $[R_{ds}](d^s) = (f_{ds})$

Section 2 : THM coupling with phase field method



- α_m : Differential expansion between rock and water
- b : Biot's coefficient
- α_{rock} : Thermal expansion coefficient of rock

Some parameters influenced by damage field d (here we only consider d^t) :

- Permeability : $k = k_0 \exp(\beta d^t)$
- Biot coefficient : $b(d^t) = b_{initial} + (1 - b_{initial})d^t$
- Porosity : $\Phi(d^t) = \Phi_{initial} + (1 - \Phi_{initial})d^t$
- Biot module : $\frac{1}{M(d^t)} = \frac{(1-b(d^t))(b(d^t)-\Phi(d^t))}{K_s} + \frac{\Phi(d^t)}{K_f}$
- Differential expansion : $\alpha_m(d^t) = (b(d^t) - \Phi(d^t))\alpha_s + \Phi_{ini}\alpha_f$

Section 3 : Thermal extension tests

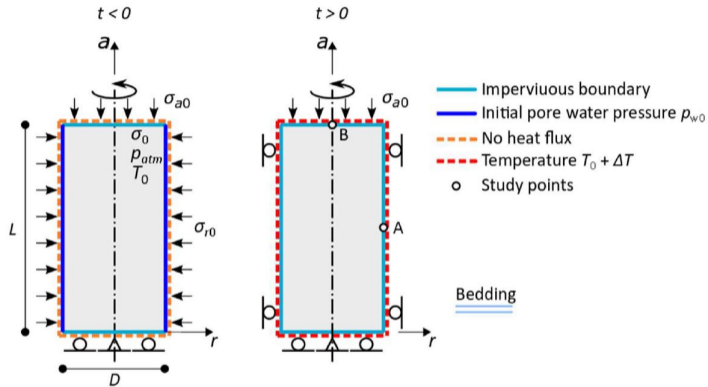
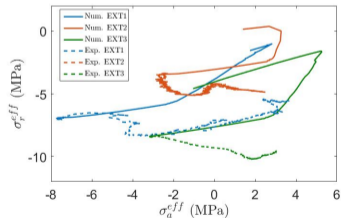
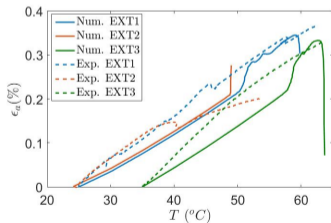
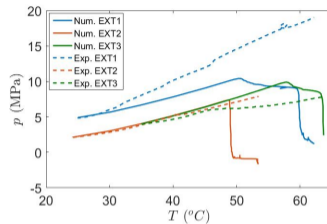
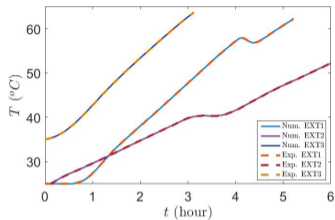


FIGURE – Modelling sequence of the thermal extension test : initial, and boundary conditions. (from Deco2023 specifications and [Braun, 2019])

Section 3 : Thermal extension tests



Section 3 : Thermal extension tests

Weibull probability distribution(WPD) for porosity f_p and inclusion fraction f_{in} :

$$f_i(x) = \frac{m}{\beta_i} \left(\frac{x}{\beta_i}\right)^{m-1} e^{-(x/\beta_i)^m}; \quad i = p, in$$

with average fraction $\beta_p = 0.18$; $\beta_{in} = 0.4$

Mori-Tanaka homogenization scheme :

Microscopic scale :

$$\mathbb{C}_{hom}^I = (1 - f_p)\mathbb{C}_0 : [(1 - f_p)\mathbb{I} + f_p(\mathbb{I} - \mathbb{P}_{hom}^I : \mathbb{C}_0)^{-1}]^{-1}$$

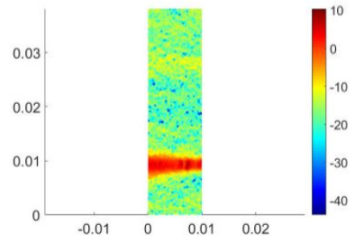
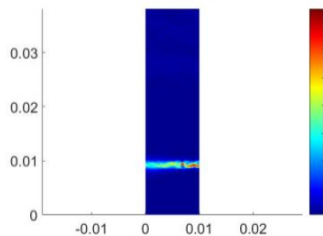
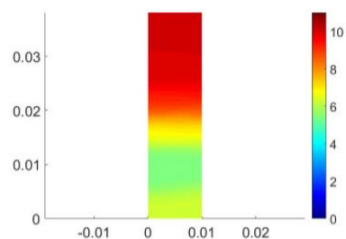
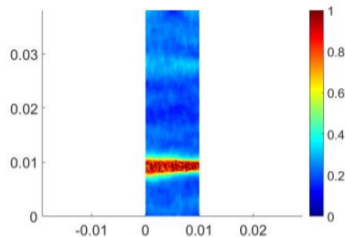
Mesosopic scale :

$$\mathbb{C}_{hom}^{II} = \mathbb{C}_{hom}^I + [f_{in}(\mathbb{C}_{in} - \mathbb{C}_{hom}^I) : \mathbb{D}_{in}] : [\mathbb{I} + f_{in}(\mathbb{C}_{in} - \mathbb{I})]^{-1}$$

Section 3 : Thermal extension tests



Photo from [Braun, 2019]



Section 3 : Excavation induced crack zone around GCS gallery

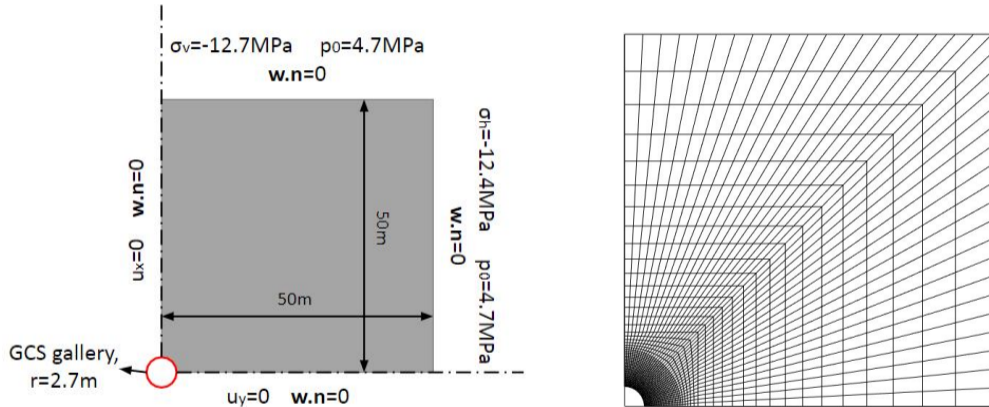


FIGURE – Boundary conditions (left) and finite element mesh (right)

Section 3 : Excavation induced crack zone around GCS gallery

Excavations take place during the 28 days :

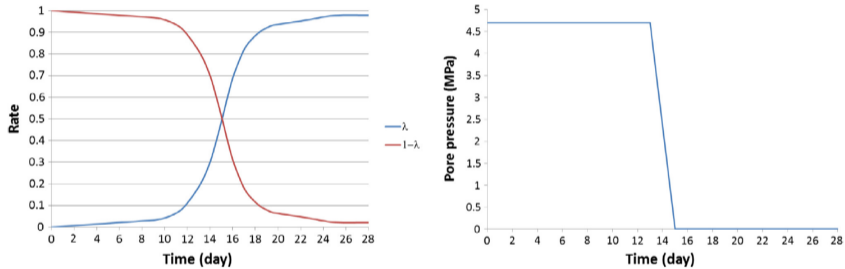
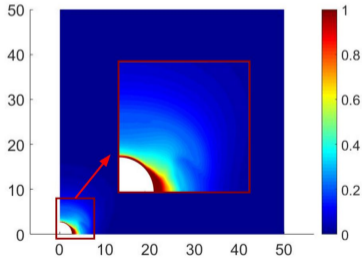
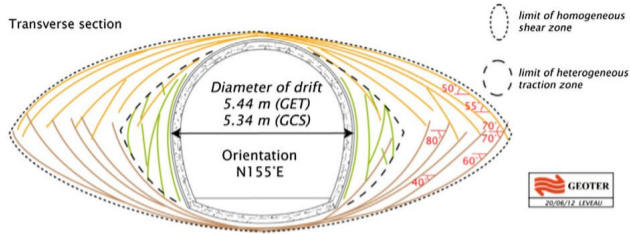


FIGURE – *Mechanical (left) and hydraulic (right) deconfinement curves.*

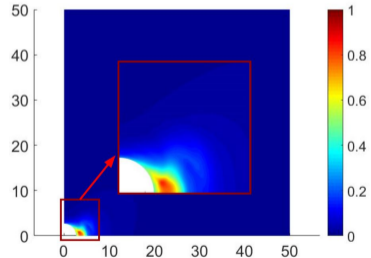
Section 3 : Excavation induced crack zone around GCS gallery

Elastic parameters	Young's modulus	$E_{\parallel}=6\text{GPa}$
		$E_{\perp}=3.5\text{GPa}$
	Poisson's ratio	$\nu_{\parallel}=0.24$
		$\nu_{\perp}=0.35$
Hydraulic parameters	Permeability	$k_{0\parallel}=6 \times 10^{-20}\text{m}^2$
		$k_{0\perp}=3 \times 10^{-20}\text{m}^2$
	Biot coefficient	$b=0.6$
	Porosity	$\Phi=0.16$
Crack fields parameters	Toughness	$g_c^t=1800\text{N/m}$
		$g_{c0}^s=4500\text{N/m}$
	Crack length	$l_d=0.1\text{m}$
	Permeability rate	$\beta=12$
	Viscoplastic effect	$\chi=0$

Section 3 : Excavation induced crack zone around GCS gallery



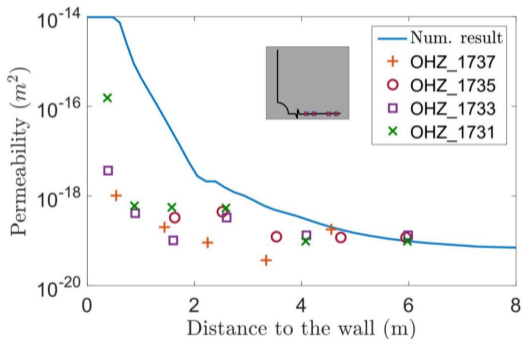
(Tensile damage)



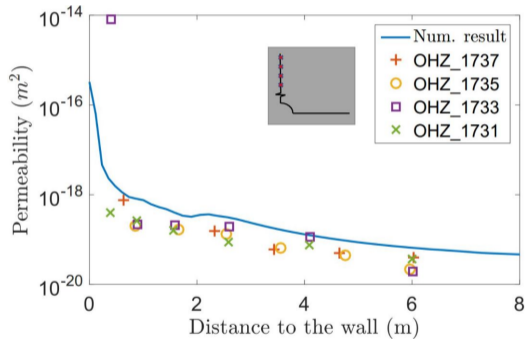
(Shear damage)

Section 3 : Excavation induced crack zone around GCS gallery

Permeability : $k = k_0 \exp(\beta d^t)$



(Horizontal direction)



(Vertical direction)

Section 3 : Excavation induced crack zone around GCS gallery

Pore pressure :

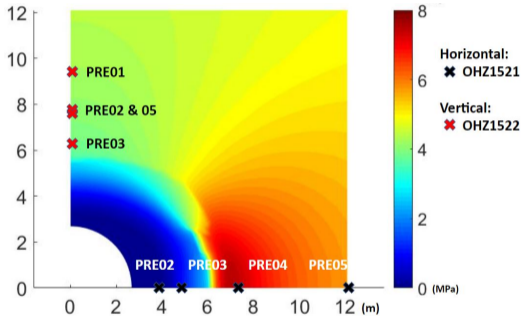
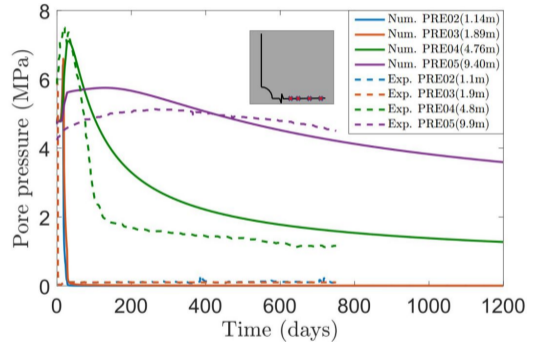
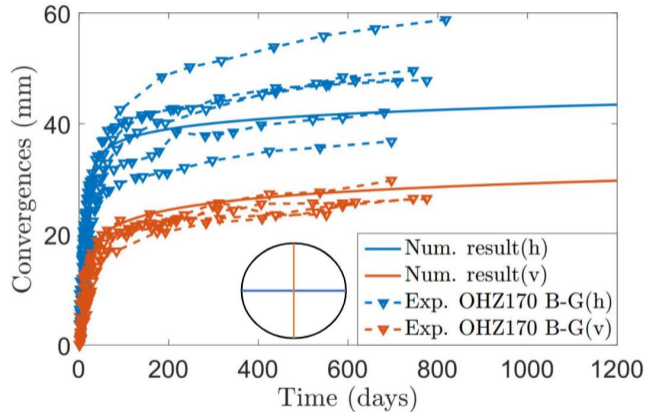


FIGURE – Distribution of pore pressure at end of excavation ($t=28$ days)



Section 3 : Excavation induced crack zone around GCS gallery



Section 3 : ALC heating test, heating induced cracking

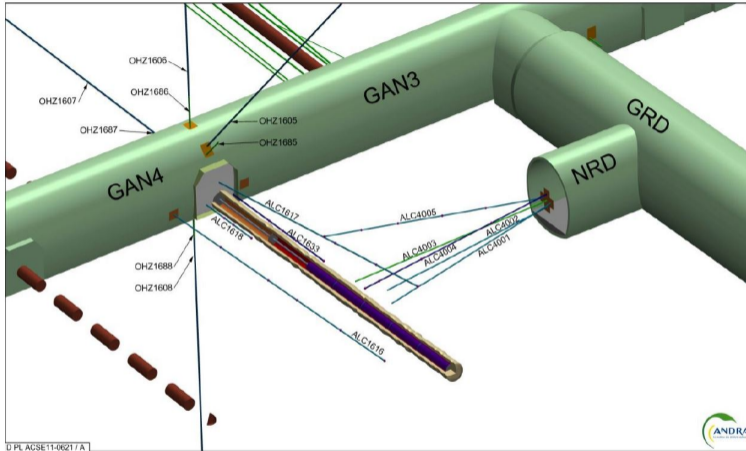


FIGURE – General view of the ALC heating experiment

Section 3 : ALC heating test, heating induced cracking

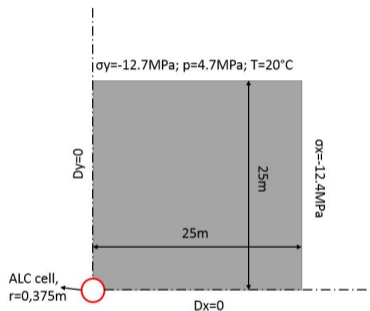


FIGURE – Modeling domain of the alveolus in 2D plane strain

Elastic parameters :

- $E_{\parallel} = 6\text{GPa}$; $E_{\perp} = 3\text{GPa}$; $\nu_{\parallel} = 0.2$;
 $\nu_{\perp} = 0.35$.

Hydraulic parameters :

- Permeability : $k_{initial\parallel} = 6 \times 10^{-20}\text{m}^2$;
 $k_{initial\perp} = 3 \times 10^{-20}\text{m}^2$.

Thermal parameters :

- Thermal conductivity :
 $\lambda_{\parallel} = 2\text{W}\cdot\text{m}^{-1}\cdot\text{K}^{-1}$;
 $\lambda_{\perp} = 1.33\text{W}\cdot\text{m}^{-1}\cdot\text{K}^{-1}$.

Section 3 : ALC heating test, heating induced cracking

The time step size used in this example :

- 0-1 day (excavation) : 1 hour
- 1-176 days : 1 day
- 176-186 days (heating starting at 176 day) : 1 hour
- 186-2500 days : 1 day

Section 3 : ALC heating test, heating induced cracking

Temperature results :

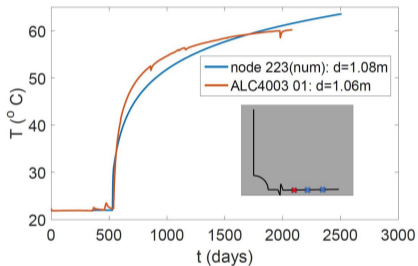


FIGURE – Temperature evolution in ALC4003, sensor 01, $d=1.06\text{m}$

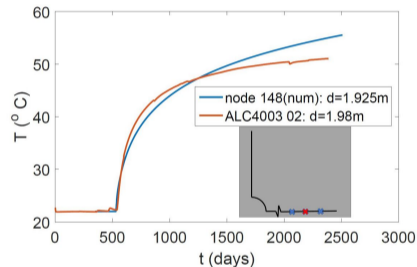


FIGURE – Temperature evolution in ALC4003, sensor 02, $d=1.98\text{m}$

Section 3 : ALC heating test, heating induced cracking

Pore pressure in horizontal direction :

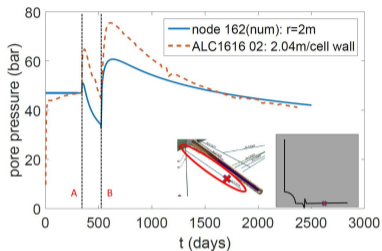


FIGURE – Pressure evolution in ALC1616 (horizontal)

Time A : Excavation ; Time B : Heating.

- Excavation induced over-pressure not correctly reproduced
 - Reasons : 3D geometrical effect, etc...
- Over-pressure due to heating almost well reproduced

Section 3 : ALC heating test, heating induced cracking

Pore pressure in vertical direction :

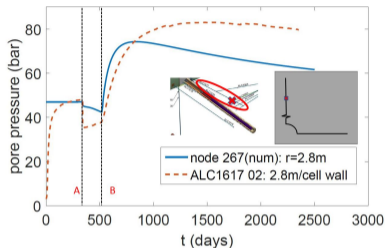


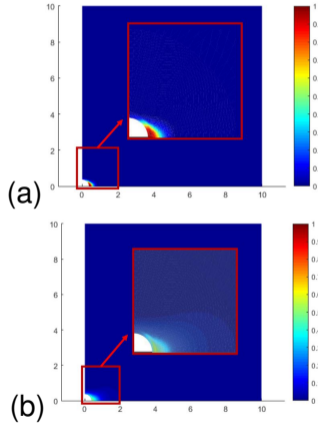
FIGURE – Pressure evolution in ALC1617 (vertical)

Time A : Excavation ; Time B : Heating.

- Excavation induced pressure decrease not correctly reproduced
 - Reasons : 3D geometrical effect, etc...
- Pressure increase due to heating quite well reproduced, but too early cooling process started

Section 3 : ALC heating test, heating induced cracking

Excavation induced damage :



Photos of cracks around the ALC :

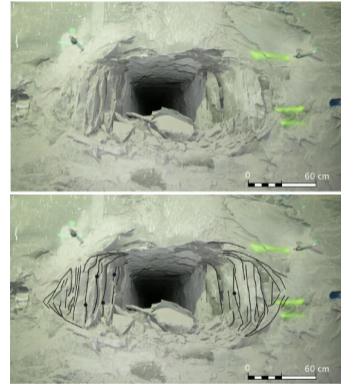


FIGURE – *Distribution of (a) tensile and (b) shear cracks at $t=1$ day*

Section 3 : ALC heating test, heating induced cracking

Excavation induced damage :

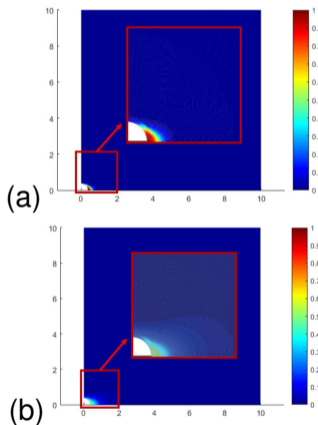


FIGURE – Distribution of (a) tensile and (b) shear cracks at $t=1$ day

Heating induced damage :

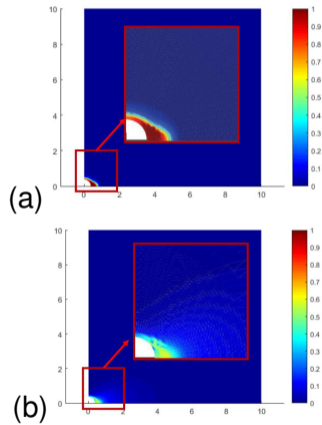


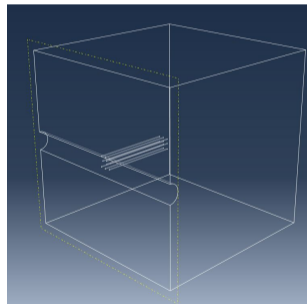
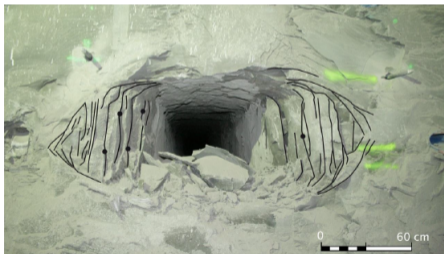
FIGURE – Distribution of (a) tensile crack and (b) shear crack at $t=1176$ days

Conclusion :

- A new modified phase field method ;
 - It is possible to consider tensile and shear damage.
- Thermal extension tests
 - The tendencies of pore pressure, strain and stress are well reproduced ;
 - The crack path is well reproduced.
- Application of GCS test
 - The pore pressure variation is well reproduced ;
 - The convergences of diameter are well reproduced ;
 - The distributions of tensile and shear damage are reproduced.
- Application of ALC test
 - The temperature variation is well reproduced ;
 - The pore pressure's changing tendency is well reproduced ;
 - The distributions of tensile and shear damage are reproduced.

Future work :

- Consider heterogeneity of materials in structure simulation
- 3D extension



Thank you for your attention !